REVIEW

Transcranial Doppler ultrasound in neurocritical care

Pablo Blanco[1] · Anselmo Abdo-Cuza[2]

Abstract
Multimodality monitoring is a common practice in caring for neurocritically ill patients, and consists mainly in clinical assessment, intracranial pressure monitoring and using several imaging methods. Of these imaging methods, transcranial Doppler (TCD) is an interesting tool that provides a non-invasive, portable and radiation-free way to assess cerebral circulation and diagnose and follow-up (duplex method) intracranial mass-occupying lesions, such as hematomas and midline shift. This article reviews the basics of TCD applied to neurocritical care patients, offering a rationale for its use as well as tips for practitioners.

Keywords Transcranial Doppler · Critical care · Ultrasound · Brain injury · Point-of-care-ultrasound

Sommario
Il monitoraggio multimodale è una pratica comune nella cura dei pazienti neurocritici consistente principalmente nella valutazione clinica, nel monitoraggio della pressione intracranica e nell'utilizzo di varie tecniche di immagine. Tra queste ultime il Doppler Transcranico (DTC), è certamente importante essendo una metodica non invasiva, portatile e non soggetta all'utilizzo di radiazioni ionizzanti per la valutazione della circolazione cerebrale e per la diagnosi e il monitoraggio di lesioni occupanti spazio come gli ematomi e di deviazione della linea mediana. In questo lavoro sono riassunti i principi di base del DTC applicato ai pazienti neurocritici, viene analizzato il razionale di utilizzo della metodica e sono forniti suggerimenti pratici per l'esecuzione dell'esame.

Abbreviations

ICP	Intracranial pressure
TCD	Transcranial Doppler
TCCS	Transcranial color-coded duplex sonography
POCUS	Point-of-care ultrasound
ICA	Internal carotid artery
MCA	Middle cerebral artery
ACA	Anterior cerebral artery
VA	Vertebral artery
BA	Basilar artery
SV	Peak systolic velocity
DV	End-diastolic velocity
MV	Mean velocity
PI	Pulsatility index
RI	Resistive index
CBF	Cerebral blood flow
OA	Ophthalmic artery
LI	Lindegaard index
ECA	External carotid artery
ONSD	Optic nerve sheath diameter

✉ Pablo Blanco
ohtusabes@gmail.com

Anselmo Abdo-Cuza
aaabdo@infomed.sld.cu

1 Ecodiagnóstico-Centro de Diagnóstico por Imágenes, 3272, 50 St., 7630 Necochea, Argentina

2 Centro de Investigaciones Médico-Quirúrgicas, 11-13 and 216 St., Siboney, 12100 Havana, Cuba

Introduction

In neurocritically ill patients, multimodality monitoring is of mainstay importance, because clinical examination alone is fairly insensitive to the following disease progression or detecting clinical deterioration [1–3].

While invasive intracranial pressure (ICP) assessment is considered a standard tool [4, 5] and is widely used, this procedure is not exempt from risks, principally bleeding and

infections, as well as the possibility of erroneous readings and the consequent inappropriate treatments [6, 7]. In these circumstances, other methods, especially non-invasive ones, are of special interest for complementing neuromonitoring.

Rune Aaslid's [8] introduction of transcranial Doppler (TCD) in 1982 constitutes an important step for non-invasive bedside study of intracranial artery flow. For this purpose, using a low-frequency ultrasound probe (e.g., 2 MHz) over specific insonation windows, it is possible to gain access to the arteries that shape the Circle of Willis. Later technologic advances improved the ease and availability of the method, as well as extended its applications: for example, the introduction of color M-mode to conventional TCD, transcranial color-coded sonography (TCCS), three-dimensional TCCS and contrast-enhanced TCD [9, 10].

This review article focuses on the hemodynamic applications of TCD in neurocritically ill patients and discusses the main uses of TCCS.

Technology

TCD is performed in two main ways: traditional non-imaging or "blind" TCD; and TCCS. Table 1 provides a comparison between these techniques. Figure 1 shows the equipment used for performing each method. Although there are no formal recommendations regarding the selection of one method over the other, TCCS is gaining acceptance because it uses the same ultrasound machine and transducer common to general critical care US (i.e., point-of-care ultrasound or POCUS).

Generalities of the TCD study

For obtaining access to cerebral circulation, a low frequency ultrasound probe (2 MHz in average) is placed over the insonation windows (Fig. 2) [11], such as the transtemporal, transforaminal, transorbital and transcervical windows. The transtemporal window allows recognition of anterior cerebral circulation [the intracranial internal carotid artery (ICA), carotid siphon, middle cerebral artery (MCA) and anterior cerebral artery (ACA)], while the transforaminal window is used to explore posterior cerebral circulation [both the bilateral intracranial vertebral artery (VA) and the basilar artery (BA)]. The transorbital window allows the inspection of the carotid siphon as well as the ophthalmic artery. Finally, the transcervical window allows the visualization of the extracranial internal carotid artery. Of the aforementioned insonation windows, the transtemporal one is most important in practice.

The different arteries to be insonated have flows that move toward or away from the transducer (see direction of blood flow in Fig. 3) [12]. This is shown in the pulsed wave Doppler as spectrograms in the positive or negative channels, respectively. When using color Doppler or color M-mode, flows that move toward the transducer are coded in red, while flows that move away are coded in blue.

The registered doppler parameters include peak systolic velocity (SV), end-diastolic velocity (DV), mean velocity (MV) and the Doppler indices [pulsatility index (PI) and resistive index (RI)]. PI is automatically calculated as $(SV - DV)/MV$ and RI as $(SV - DV)/SV$ (Fig. 4). Velocities are dependent on the angle of insonation, while Doppler indices are not; thus, using the latter is preferable when velocities are not accurate (e.g., large insonation angles). In contrast to conventional TCD, TCCS allows

Table 1 Comparison between conventional transcranial Doppler and transcranial color-coded duplex sonography

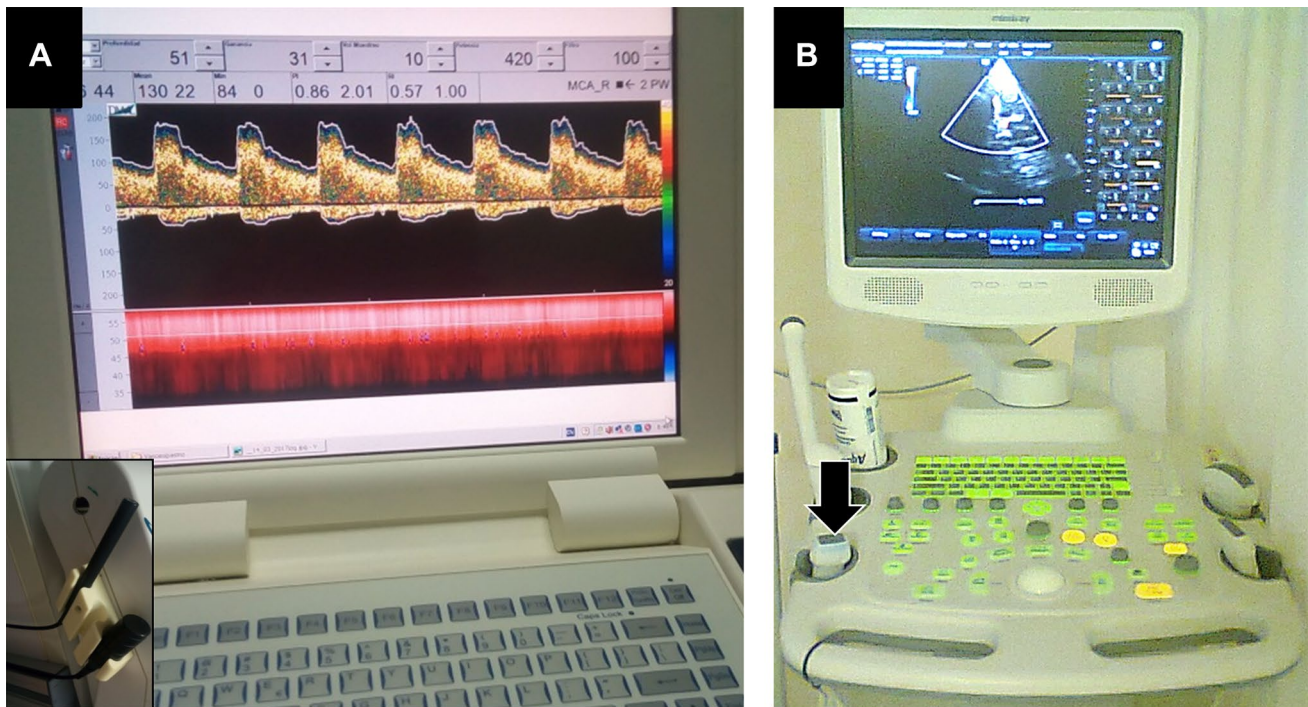|	Conventional transcranial Doppler	Transcranial color-coded duplex sonography
Machine	Dedicated	The same US machine and transducers used for general US in critically ill patients
Transducers needed	3	Mainly 1 (e.g., phased-array probe)
Spectral Doppler (hemodynamic diagnosis)	Yes	Yes
Electronic angle correction	No	Yes
Color Doppler	No (except in machines with color M-mode capabilities)	Yes
Two-dimensional imaging	No	Yes
Continuous monitoring using helmet	Yes	No
Detection of microemboli	Yes	Yes
Availability	Poor	Wide
Learning curve	Long	Probably shorter than conventional TCD

TCD transcranial Doppler, *US* ultrasound

Fig. 1 a Conventional (non-imaging or blind) transcranial Doppler equipment with color M-mode capabilities, and its transducers; **b** general ultrasound machine, where a phased array probe (arrow) is used for performing the transcranial Doppler (duplex imaging)

electronically correcting the angle of insonation and thus obtaining more accurate velocities [12]. In normal circumstances, cerebral circulation has a low resistance velocity profile on spectral Doppler. This is clearly different from the high-resistance velocity profile seen in resting striated muscle arteries or in the external carotid artery (Fig. 5).

Cerebral blood flow (CBF) running through a vessel is equal to the product of the MV and the cross-sectional area. If the area is normal and constant, CBF will be mainly dependent on variations in the MV. Thus, in this scenario, MV can be considered a surrogate of CBF. Factors affecting the MV (and thus the CBF) are, among others, age, cerebral perfusion pressure, hematocrit, core body temperature, arousal, pain, endotracheal suction and inflammation (e.g., meningitis) [12, 14]. However, when the area is reduced, as in atherosclerotic stenosis or in cerebral vasospasm, an increase in the MV is necessary to maintain the CBF, although in this case the MV is neither interchangeable nor a surrogate of the CBF. In fact, the cerebral perfusion running down the stenosis can be critically compromised, despite the recording of elevated MV. Table 2 shows the factors that can modify the Doppler velocities and indices. Due to the reasons explained above, since many variables can affect the Doppler findings and thus complicate its interpretation, it is important to perform TCD study when the mean arterial pressure is at least 60 mmHg, arterial blood gases (e.g., $PaCO_2$) and

core temperature are normal and an appropriate sedation level is achieved [13].

Conventional transcranial Doppler

In this conventional modality, the transducer is placed over the selected insonation window, obtaining Doppler signals in a blind manner at specific interrogation depths (Doppler shifts are also heard). New machines add color M-mode capabilities, allowing easier detection of flows.

The most important window is the transtemporal, found by placing the transducer above the zigomatic arch and immediately anterior to and slightly above the tragus of the ear ("pterion"). The TCD study is started at a depth of 50 mm, where it is expected to register a flow directed toward the probe (positive in the scale), corresponding to the main segment, or M1, of the MCA (Fig. 6a). Advancing up to a depth of 65 mm, a bidirectional flow is recorded (positive/negative on the scale), corresponding to the bifurcation of the ICA into the MCA and the ACA. At this point, directing the transducer slightly cephalad and anterior, the first segment, or A1, of the ACA is normally found, with its flow directed away from the probe (negative in the scale) (Fig. 6b). Returning to the ICA bifurcation, without changing the depth and with slightly caudal angulation, it is possible to register the flow of the carotid siphon moving toward
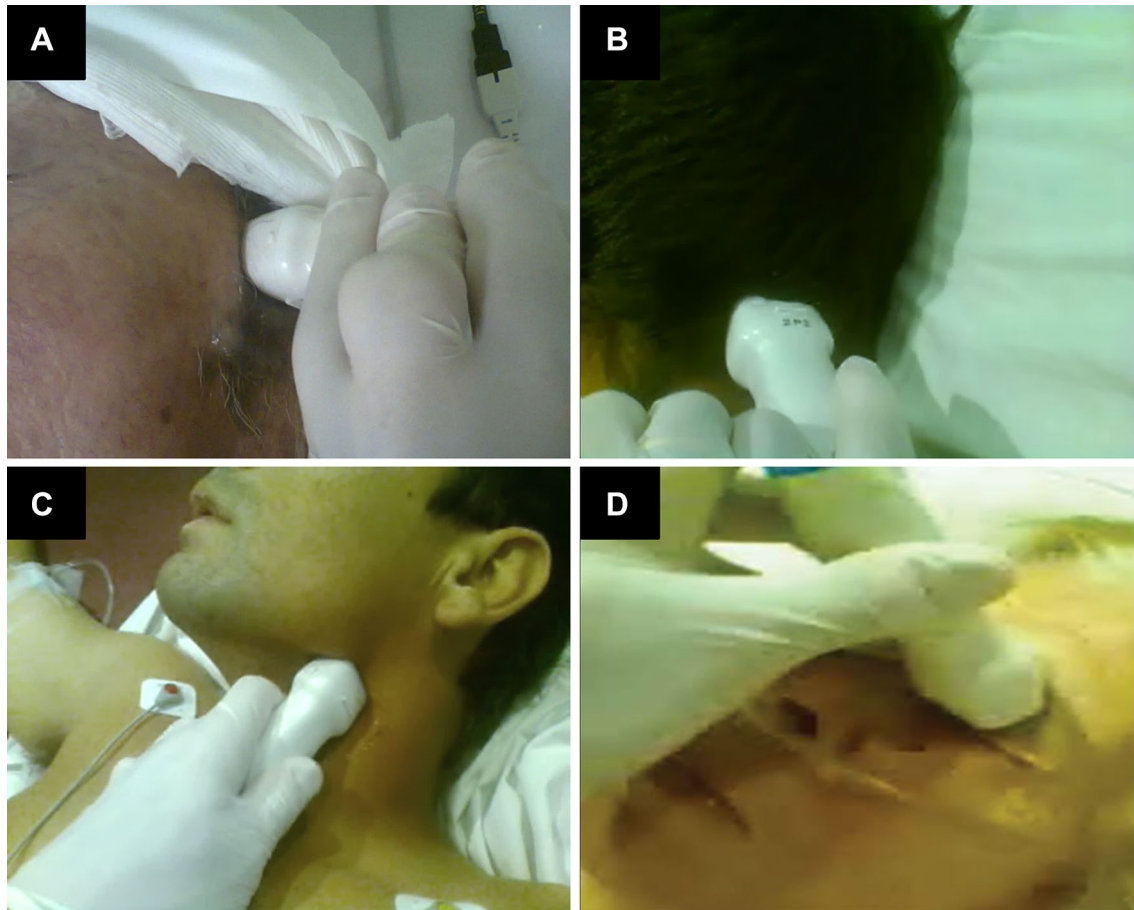
Fig. 2 Transcranial Doppler insonation windows. **a** Transtemporal; **b** transforaminal; **c** transcervical; **d** transorbital
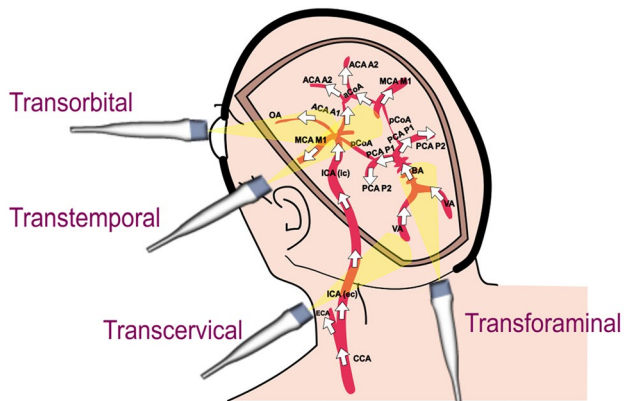

Fig. 3 Schematic view of the cerebral circulation, with normal direction of blood flow and transcranial Doppler windows. *CCA* common carotid artery, *ECA* external carotid artery, *ICA (ec)* distal extracranial internal carotid artery, *ICA (ic)* intracranial ICA, *VA* vertebral artery, *BA* basilar artery, *MCA M1* first segment of the middle cerebral artery, *ACA A1* first segment of the anterior cerebral artery, *ACA A2* second segment of the anterior cerebral artery, *aCoA* anterior communicating artery, *OA* ophthalmic artery, *pCoA* posterior communicating artery, *PCA P1* first segment of the posterior cerebral artery, *PCA P2* second segment of the posterior cerebral artery

the transducer. Using the ICA bifurcation as a starting point, and orientating the probe slightly posterior and caudal at a depth of 70 mm, reveals the flow of the first segment, or P1, of the PCA toward the probe. From this point, at 80 mm, the second segment, or P2, of the PCA is normally registered, with flow signals moving away from the transducer (Table 3) [11, 12, 14].

In some percentage of patients (20% approximately), it is not possible to obtain Doppler signals using the transtemporal approach [12]. Detection rates are worst in aged woman. In that situation, the anterior circulation (at least in part) can be evaluated using the transorbital window, where the carotid siphon is found at a depth of 80 mm, with flow moving toward or toward/away the probe. At a depth of 40 mm is the ophthalmic artery (OA), with flow typically moving toward the transducer (Table 3). In contrast to intracranial arteries, the OA has a high-resistance velocity profile [11]. Precautions should be taken into account when using the transorbital window; it is recommended to decrease the power output to 20% in order to avoid potential risks of ocular damage [15].
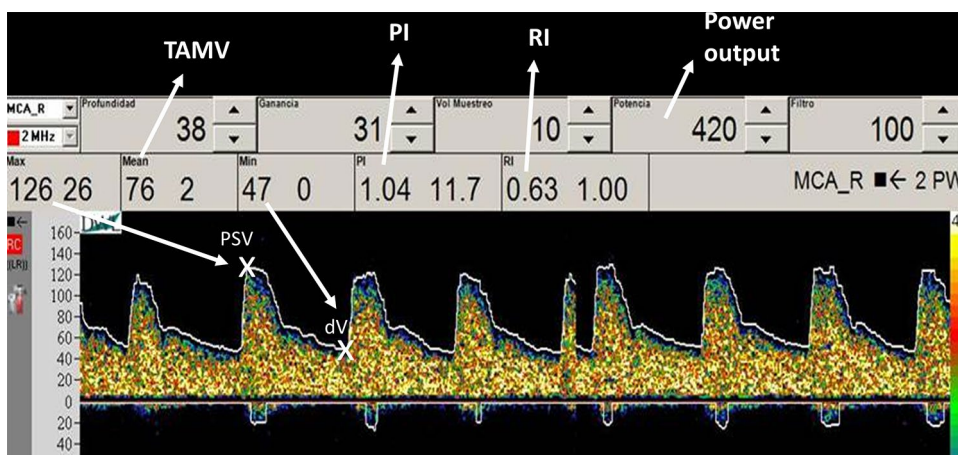
Fig. 4 Doppler waveforms registered in the middle cerebral artery (depth of 38 mm), represented in the anterograde channel. Maximum or peak systolic velocity (SV, 126 cm/s), end-diastolic velocity (DV, 47 cm/s) and time-averaged mean velocity (TAMV, or MV, 76 cm/s) are recorded. Doppler indices shown are a pulsatility index (PI), automatically calculated as $(SV - DV)/MV$, of 1.04 and a resistive index (RI), automatically calculated as $(SV - DV)/SV$, of 0.63. The power output should be lowered for the transorbital window

Fig. 5 **a** Low resistance velocity profile, corresponding to the middle cerebral artery; **b** high-resistance velocity profile, corresponding to the external carotid artery
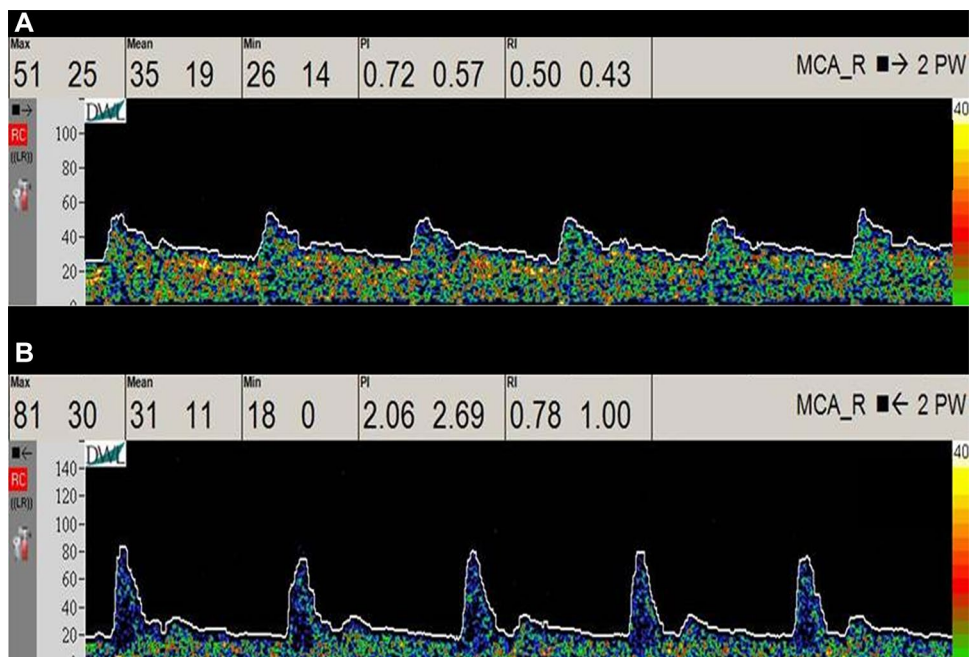

In transforaminal windows, the patient is placed in lateral decubitus, with the neck flexed so the chin touches the chest [15]. The transducer is placed along the midline below the occipital prominence and directed toward the nose. Study starts at a depth of 55 mm by slightly angulating laterally the probe to find a flow moving away from the transducer, corresponding to either one of the intracranial vertebral arteries. By increasing the depth up to 120 mm, it is possible to register the flow of the basilar artery, also directed away from the transducer (Table 3). Flow detection rates are worse than with the transtemporal window.

In the transcervical window, the probe is placed below the angle of the mandible, medial to the sternocleidomastoid muscle, and angulated upward at a depth of 40–50 mm to obtain a low resistance flow corresponding to the distal extracranial ICA (Table 3). The low resistance velocity profile of the ICA should not be confused with the high-resistance flow of the external carotid artery (ECA), which also has a sharp systolic upstroke and an early diastolic notch (see Fig. 5 above). The temporal tapping maneuver sometimes helps in difficult cases [15]. As mentioned below, the MV of the distal ICA is important for calculation of the Lindegaard

Table 2 Common factors affecting the velocities and indices on transcranial Doppler

Velocities		Doppler indices	
Increase	Decrease	Increase	Decrease
Reduced vessel area (e.g., vasospasm, atherosclerotic stenosis)	Age	Intracranial hypertension	Hypercapnia
Anemia	Hyperviscosity	Hypocapnia	Distal vasodilation down to a stenosis
Hyperemia	Dehydration	Aortic regurgitation	Hyperemia
Hyperthermia	Low cardiac output	Chronic arterial hypertension	Hypervolemia
Hypervolemia	Arterial hypotension	Leukoaraiosis	
Arterial hypertension	Hypotermia		
Hypercapnia	Sedative and hypnotic medication		
Hypoxemia			
Volatile anesthetics			

Fig. 6 **a** Doppler waveforms represented in the anterograde channel, corresponding to the M1 segment of the middle cerebral artery. **b** Doppler waveforms in the retrograde channel, corresponding to the A1 segment of the anterior cerebral artery
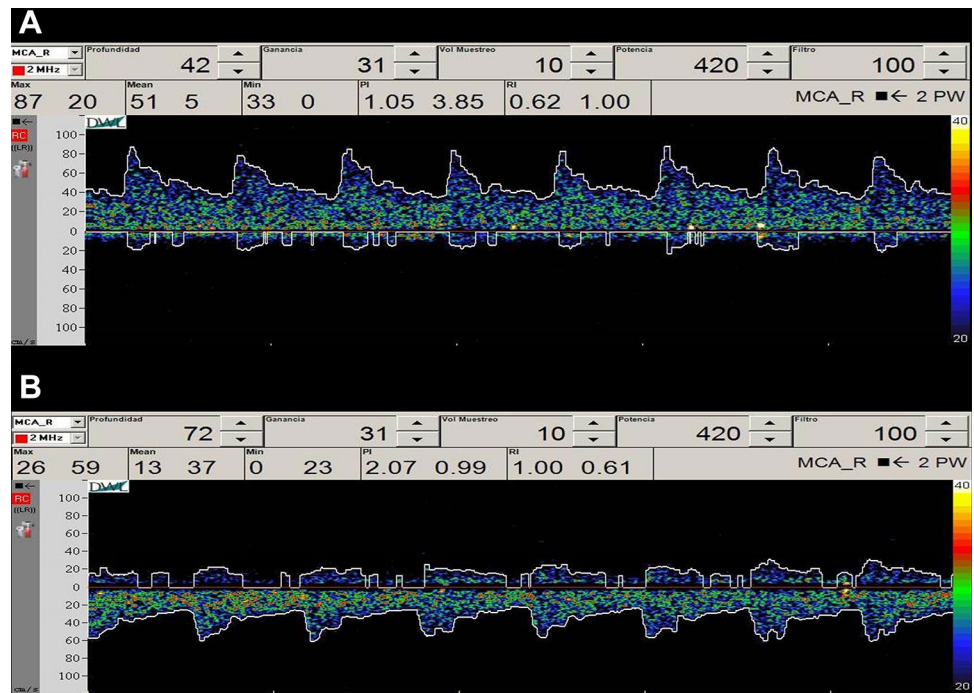
index, which contributes to distinguishing hyperemia from vasospasm [11]. Normal values of velocities and indices are provided in Table 4.

Hemodynamic patterns recognized by transcranial Doppler

There are some controversies regarding the value of TCD for assessment of cerebral perfusion, probably due to the many variables that affect Doppler parameters (see Table 2). TCD findings must be integrated into the patient's context and thus caution should be exercised when interpreting its values in an isolated manner. Of note, trends are more important than isolated values and thus helpful in the diagnostic process.

The following hemodynamic patterns can be described using TCD [16, 17]:

Normal

MV and PI within normal reference values [18].

Hypoperfusion or low flow

It is defined as the velocities below the normal reference values with or without elevation of the Doppler indices. Ract et al. [19] defined hypoperfusion as when MV < 30 cm/s, DV < 20 cm/s and PI > 1.4 (Fig. 7).

Table 3 Window, depth, flow direction and spectral Doppler coding in conventional transcranial Doppler. Modified from [15]

Artery	Window	Depth (mm)	Flow direction in relation to the probe	Coding in the scale
MCA, main segment or M1	Transtemporal	30–55	Toward	Positive
ICA bifurcation into MCA and ACA	Transtemporal	55–65	Toward/away	Positive/negative
ACA A1	Transtemporal	60–80	Away	Negative
PCA				
P1 or precommunicating	Transtemporal	60–70	Toward	Positive
P2 or postcommunicating		80	Away	Negative
Vertebral artery	Transforaminal	55	Away	Negative
Basilar artery	Transforaminal	60–80	Away	Negative
Extracranial ICA	Transcervical	40–50	Away	Negative
Carotid siphon	Transorbital	60–80	Toward or	Positive or
			Toward/away	Positive/negative
	Transtemporal	55–65	Toward	Positive
Ophtalmic artery	Transorbital	40	Toward	Positive

MCA middle cerebral artery, *ICA* internal carotid artery, *ACA* anterior cerebral artery, *PCA* posterior cerebral artery

Table 4 Reference values of velocities and Doppler indices on transcranial Doppler. Modified from [15]

Artery	Systolic velocity (cm/s)	Diastolic velocity (cm/s)	Mean velocity (cm/s)	Pulsatility index	Resistive index
ACA	80–90	30–40	50–60	0.72–0.92	0.53–0.59
MCA	90–110	35–55	55–80	0.81–0.97	0.54–0.62
PCA	66–81	26–33	42–53	0.78–0.97	0.53–0.60
BA	54–74	23–34	35–50	0.77–0.95	0.51–0.60
VA	52–66	22–31	33–44	0.78–0.94	0.53–0.59
OA			20–30	> 1.2	

ACA anterior cerebral artery, *MCA* middle cerebral artery, *PCA* posterior cerebral artery, *BA* basilar artery, *VA* vertebral artery, *OA* ophthalmic artery
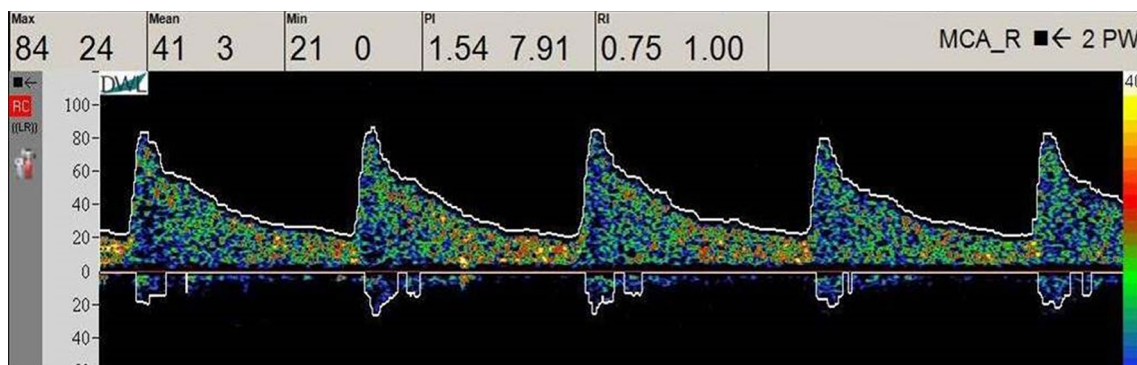

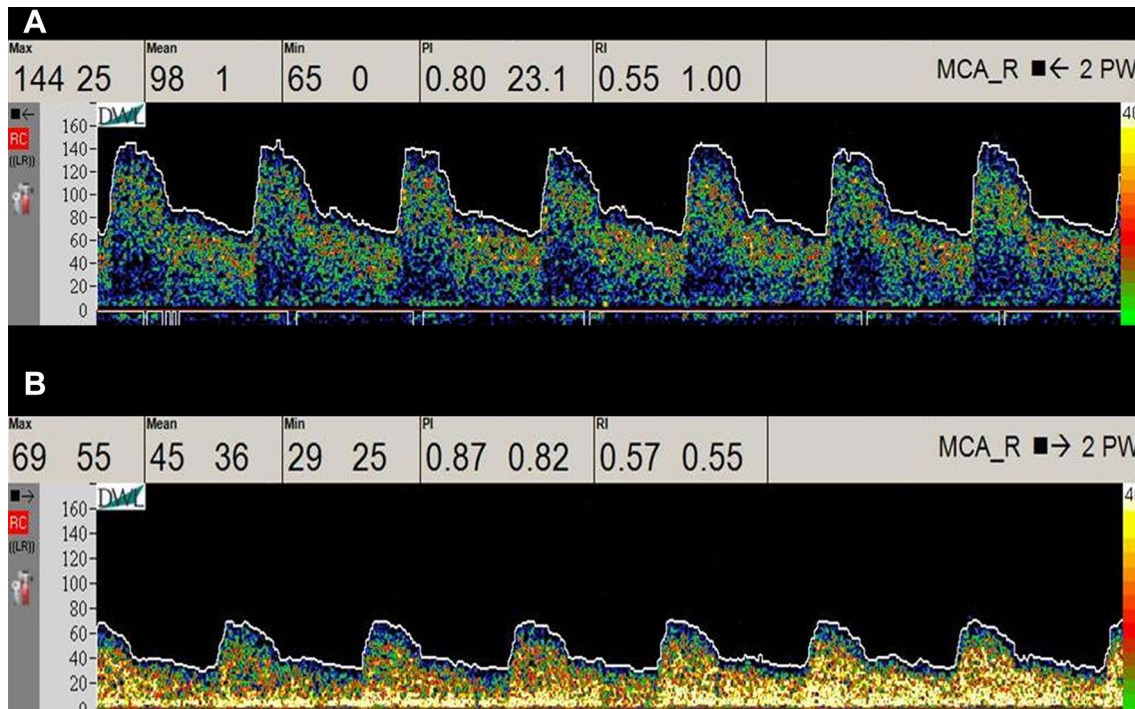**Fig. 7** Low flow pattern registered in the MCA

Fig. 8 Hyperemia. **a** Doppler waveform obtained in the MCA; **b** Doppler waveform corresponding to the distal extracranial internal carotid artery (transcervical windows). The Lindegaard index is the MV in MCA/MV in the ICA (98/45) and is equal to 2.1, indicating hyperemia
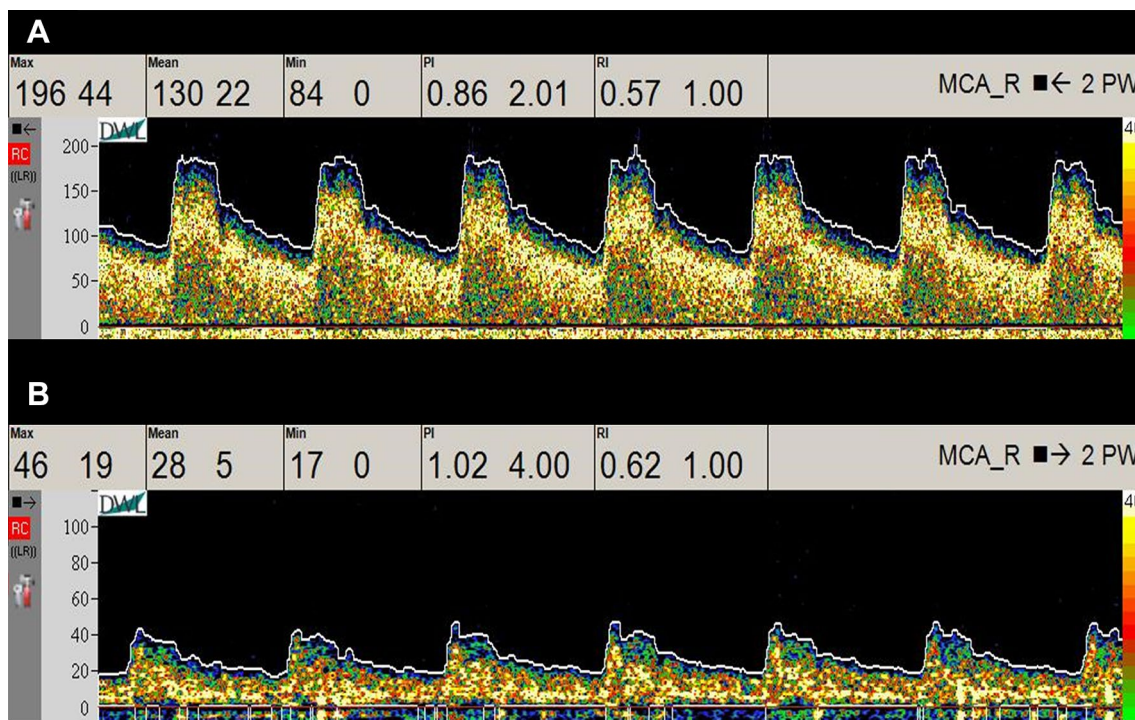

Fig. 9 Vasospasm. **a** Doppler waveform obtained in the MCA; **b** Doppler waveform corresponding to the distal ICA (transcervical windows). The Lindegaard index is MV in MCA/MV in the ICA (130/28) and is equal to 4.6, indicating vasospasm
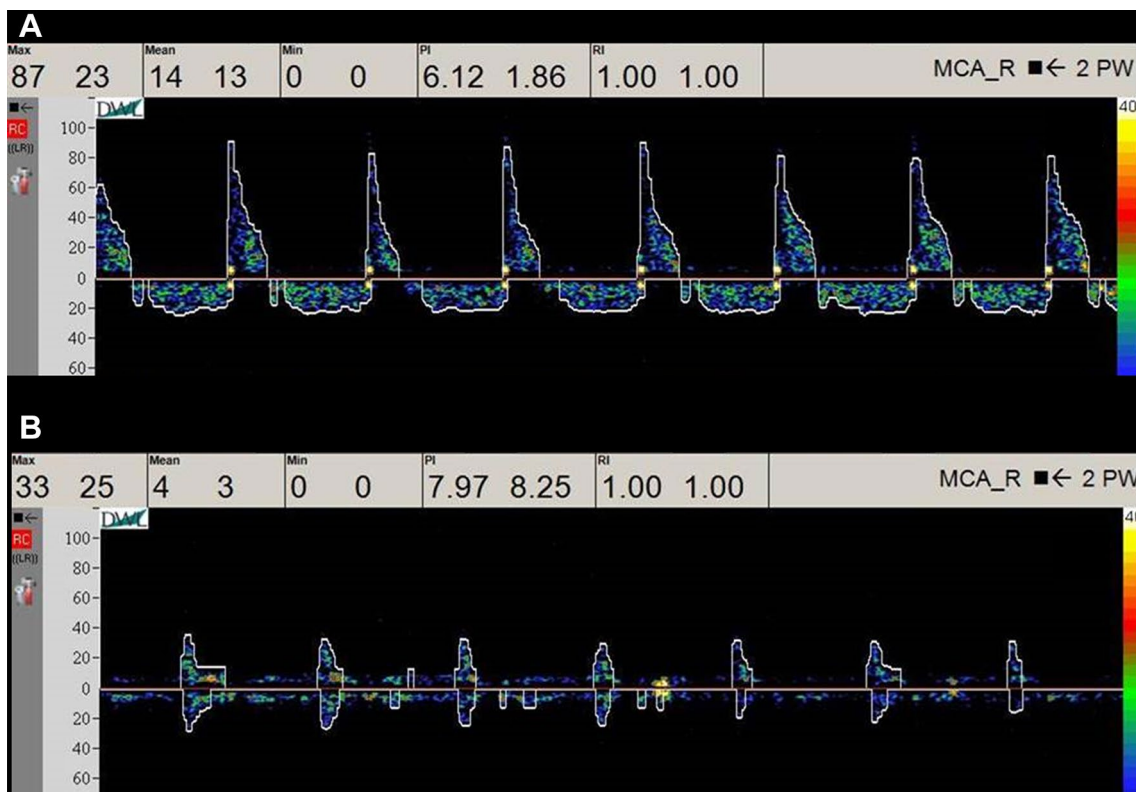
Fig. 10 Cerebral circulatory arrest patterns. **a** Reverberating or oscillating patterns; **b** systolic spikes. Note that the reverberating pattern is a biphasic flow with a net flow of zero (in contrast with a biphasic high-resistance pattern with net anterograde flow > 0)

Hyperemia and vasospasm

It is defined as the velocities above the normal reference values. To distinguish from vasospasm or other stenosis, hyperemia is defined when the Lindegaard index of the anterior circulation (MV MCA/MV extracranial ICA)

Table 5 Differential diagnosis according to the main hemodynamic pattern detected on TCD

Hemodynamic pattern	Differential diagnosis
Hypoperfusion with normal PI	Cerebral infarction Metabolic encepalopathy
Hypoperfusion with high PI	Low CPP (low MAP, high ICP or both) Hypocapnia Hypothermia
Hyperemia	Sepsis (high cardiac output) Reperfusion after cardiac arrest Meningitis Anemia Hypercapnia Fever
Vasospasm	Subcarachnoid hemorrage Vasculitis Intracranial artery stenosis
High resistance	Early rise in ICP Older age
Cerebral circulatory arrest	Re-bleeding after subcarachnoid hemorrhage Transient rise in ICP Cardiac circulatory arrest

PI pulsatility index, *MAP* mean arterial pressure, *ICP* intracranial pressure, *CPP* cerebral perfusion pressure

Table 6 TCD-guided interventions

Hypoperfusion	Hyperemia	Vasospasm
Improve the CPP	Identify and correct anemia	Nimodipine, 60 mg every 4 h
Rise the MAP: fluids or vasoactives		Rise MAP (normal saline boluses and/or vasoactives)
Decrease the ICP: ventricular drainage, osmotic therapy, transient hyperventilation	Hypercapnia	Planning cerebral angiography
	Fever	
Both	Seizures	
Planning CT	Sepsis	

ICP intracranial pressure, *CPP* cerebral perfusion pressure, *MAP* mean arterial pressure, *CT* cranial computed tomography

is < 3; while vasospasm when the LI is > 3 (Figs. 8 and 9). The Lindegaard index of the posterior circulation is also described, with the ratio of the MV BA and the extracranial vertebral artery, or the ratio of the intracranial VA and the extracranial VA, since vasospasm can also occur in these vessels. An LI < 2 suggests hyperemia, while > 2 indicates vasospasm.

High resistance

It is defined as the PI above reference values with normal velocities. This pattern is observed not only in the initial phases of increased ICP, but also in non-pathological circumstances.
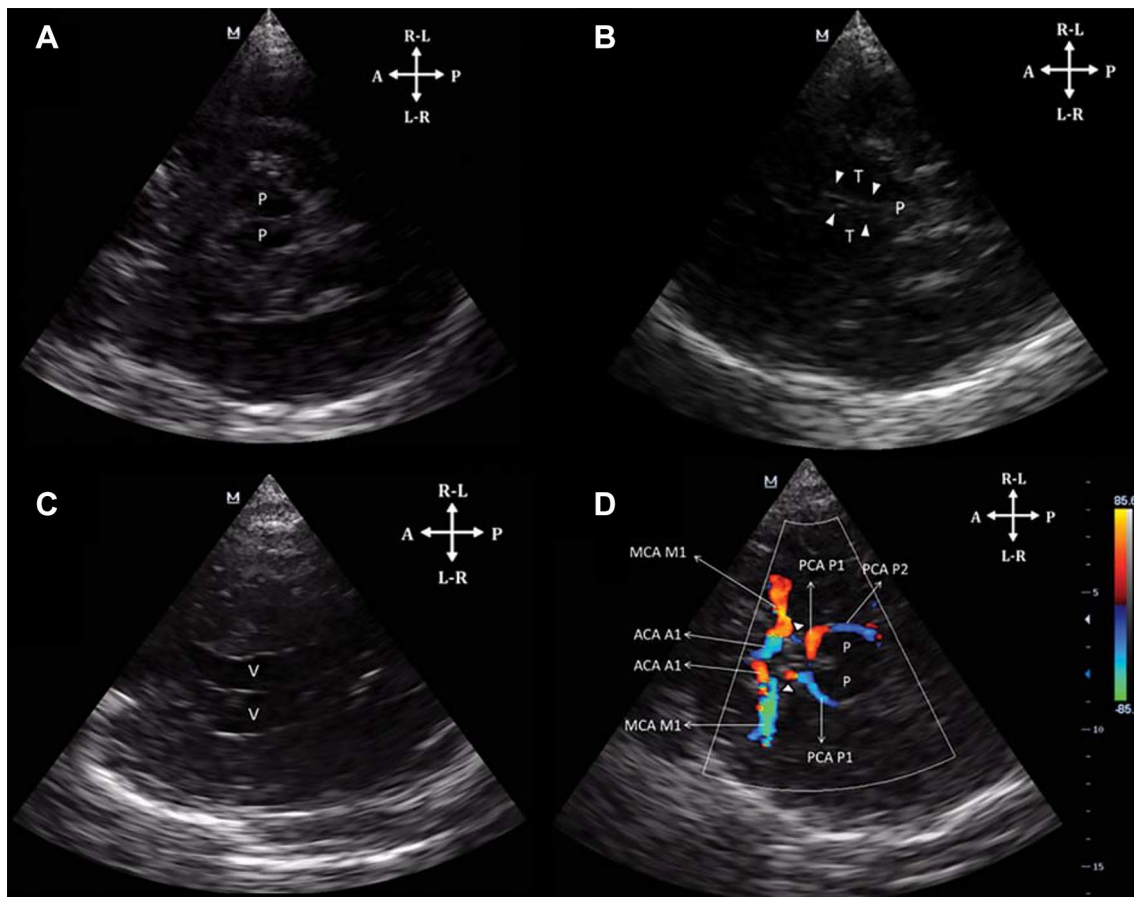

Fig. 11 a TCCS from a transtemporal view on the mesencephalic plane. *P* cerebral peduncles; **b** TCCS from a transtemporal view on the diencephalic plane. The double hyperechoic line corresponds to the third ventricle (arrowheads); *T* thalami, *P* pineal gland. **c** TCCS from a transtemporal view on the ventricular plane. Both lateral ventricles (v) are visualized. **d** Color Doppler demonstrating the vessels of the Circle of Willis. *ACA* anterior cerebral artery, *A1* precommunicating, *MCA* middle cerebral artery, *M1* mainstem; PCA: posterior cerebral artery with P1: precommunicating and P2: postcommunicating segments. Posterior communicating arteries (arrowheads) (Reproduced with permission from [25])
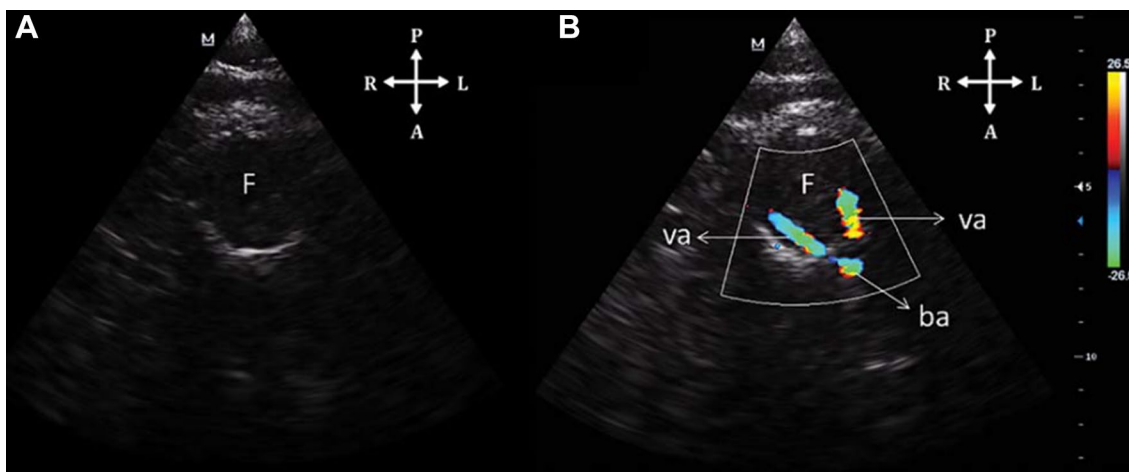
Fig. 12 TCCS from a transforaminal view. **a** Two-dimensional imaging. *F* hypoechoic foramen magnum, **b** Color Doppler showing the V-shaped artery configuration of posterior cerebral circulation. *va* vertebral arteries, *ba* basilar artery, *F* foramen magnum (Reproduced with permission from [25])
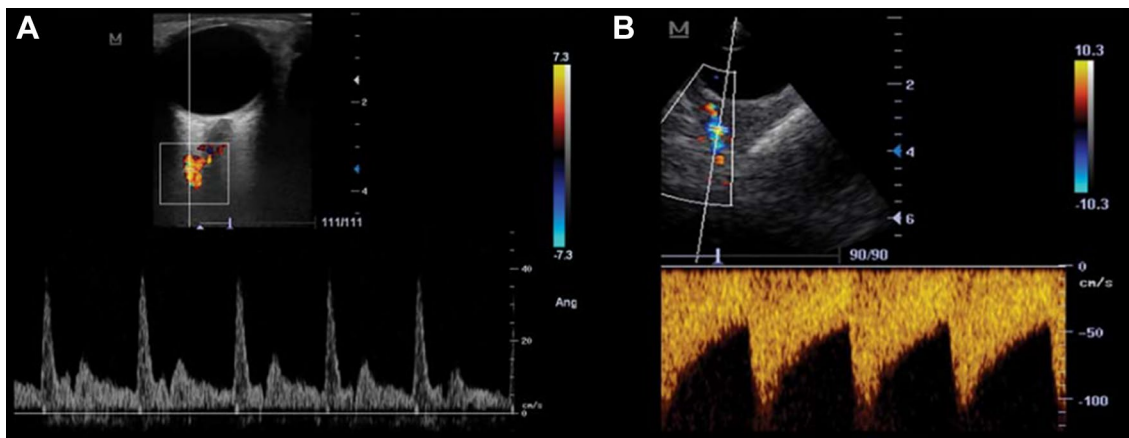

Fig. 13 TCCS from a transorbital view. **a** Linear probe. Note the normal ophthalmic artery flow toward the transducer in both color and spectral Doppler. **b** Phased array probe. Note the retrograde ophthalmic artery flow, both in color and spectral Doppler (negative in scale at right), away from transducer. This flow profile indicates near or occlusion of ipsilateral internal carotid artery and compensatory flow through collaterals of the ipsilateral external carotid artery (**a** Reproduced with permission from [25])

Cerebral circulatory arrest

It is defined as the presence of reverberating flow, systolic spikes or the disappearance of previously registered Doppler flow signals [11, 14]. To define this diagnosis, the recording of these patterns in both the anterior circulation (MCA) and posterior circulation (BA, intracranial vertebral arteries) is desirable (Fig. 10). To confirm the irreversibility of the CCA, two readings 30 min apart must show the described patterns. When the MCA and BA/VA flows are not detected, transorbital insonation of the ICA and extracranial interrogation of the ICA or the vertebral arteries may display the same CCA patterns, although it is noted that these signals appear later compared to the MCA or BA. False positives are found in subarachnoid hemorrhage with a sudden rise in ICP, transient rises in ICP and in cardiac circulatory arrest. False negatives can be found in cases of loss of skull hermeticity, such as in fractures, decompressive craniectomy and ventriculostomy [20].

Table 5 shows the main TCD hemodynamic patterns and differential diagnosis.

Decision-making process according to the TCD pattern

When detecting new hemodynamic alterations using TCD, it is of paramount importance to correlate TCD with ICP readings and clinical or other imaging data to avoid
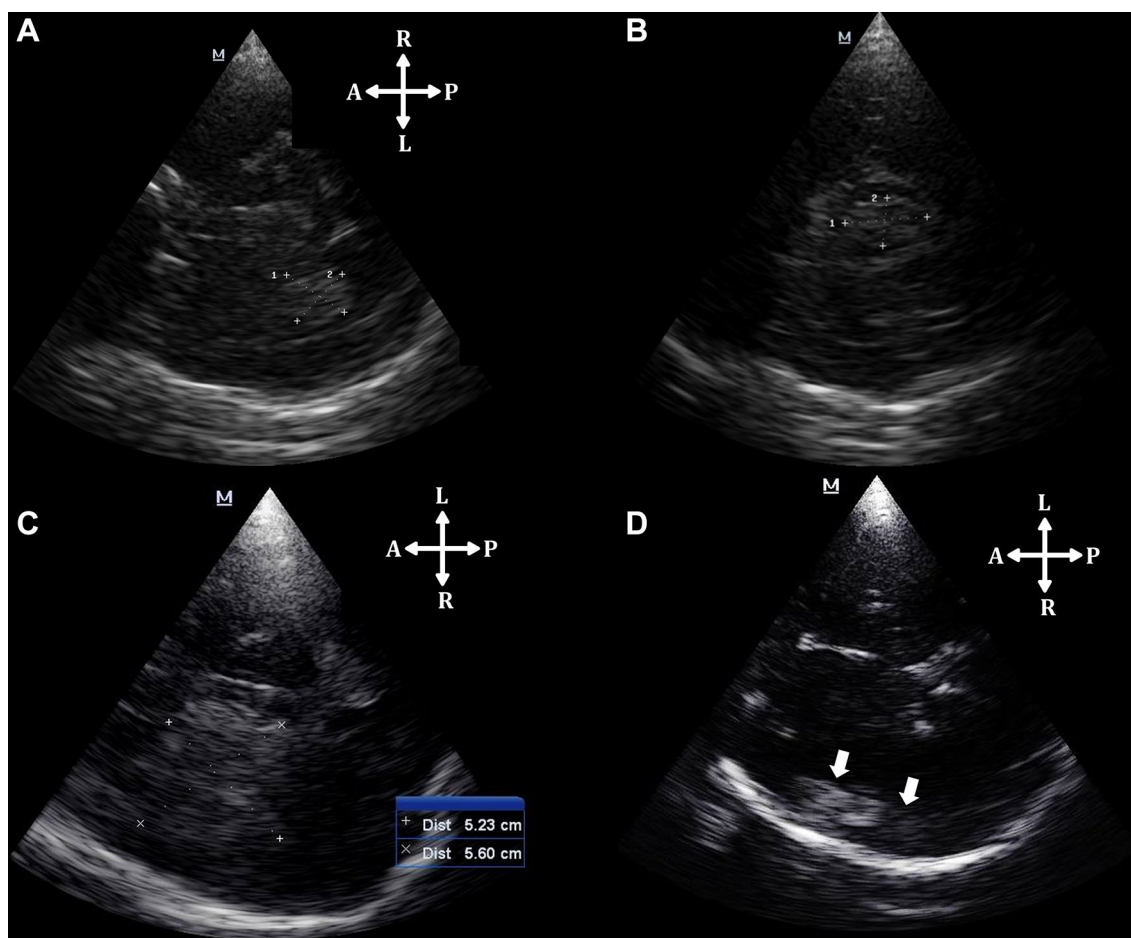
Fig. 14 Acute hematomas on TCCS. **a** Left intraparenchymal hematoma (calipers); **b** mesencephalic hematoma (calipers); **c** large right intraparenchymal hematoma (calipers); **d** right extra-axial hematoma (arrows) (Reproduced with permission from [27])

misinterpretation. As previously mentioned, trends are better than isolated values; thus, performing repeated TCD readings or eventually using a continuous monitoring system (e.g., helmet) are encouraged. When it is clear that hemodynamic alterations are not transient, repeating the cranial CT or other imaging techniques (e.g., angiography) is usually mandatory. However, these practices are not risk free, because they require translating an unstable patient to the radiology department. Since neurocritical care patients usually require immediate interventions, some of these can be started with the data provided by TCD, allowing temporary deferral of moving the patient until a safer time. Table 6 shows some TCD-guided interventions that can be performed at the bedside.

Limitations of conventional TCD

The main limitations of TCD are its operator dependency and the presence of adequate insonation windows [12].

Another limitation is the possibility of registering inaccurate velocities due to wrong insonation angles (lower than 20° are acceptable). Contrast-enhanced ultrasound (CEUS), proven to improve ultrasound accuracy in several fields [21–23], may also improve detection of flows in non-conclusive TCD [24], although its main limitations are availability and cost.

Transcranial color-coded duplex sonography

TCCS is poorly known and thus underutilized in neurocritical care. TCCS is performed using the same equipment as general ultrasound in critically ill patients, and the same transducer as transthoracic echocardiography (i.e., phased array probe). TCCS uses the same insonation windows as TCD. In addition to the hemodynamic diagnosis common to TCD, this modality provides two-dimensional imaging of intracranial structures, as well as color Doppler depiction of the relevant vasculature, allowing faster and easier finding of the arteries [15, 25]. Another advantage is the correction
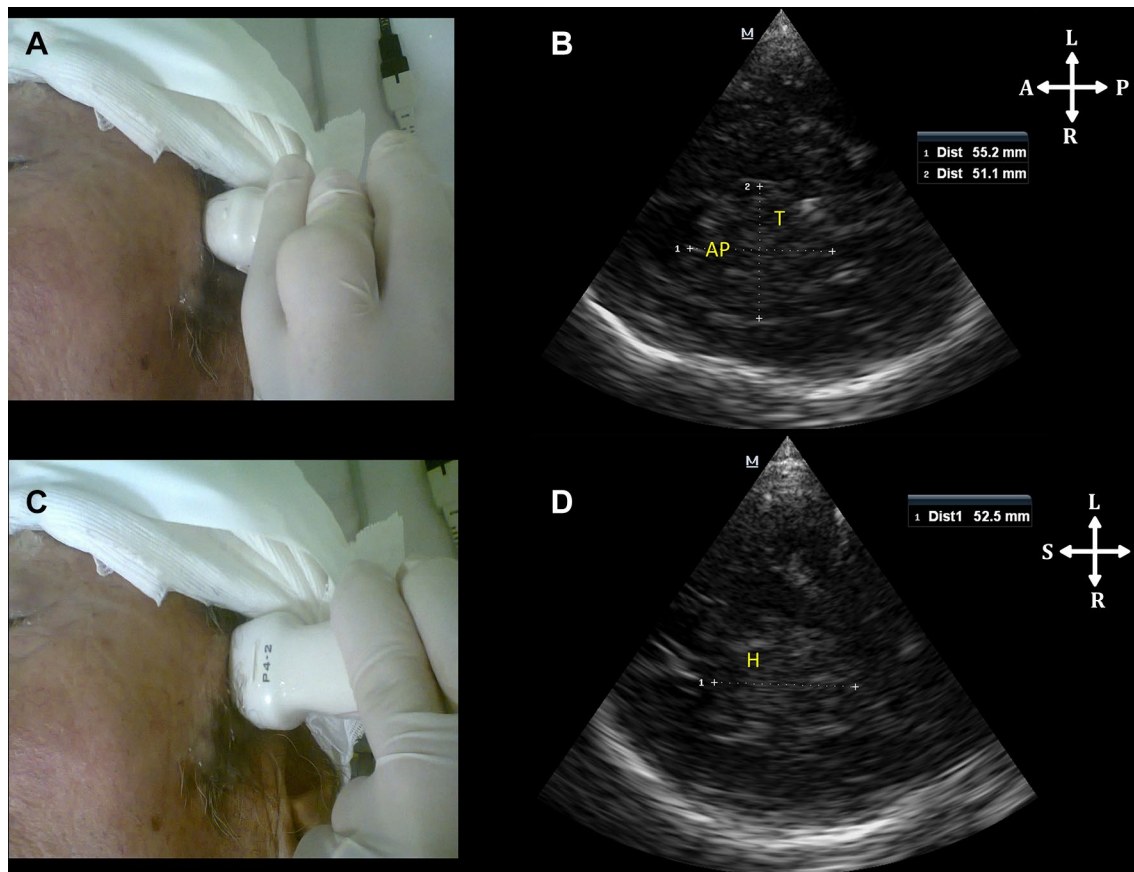
Fig. 15 Measurement of the hematoma volume by TCCS. **a**, **b** Transtemporal axial plane. The anteroposterior (AP, 1: 5.5 cm) and transverse (*T*, 2: 5.1 cm) diameters are measured. **c**, **d** Transtemporal coronal plane. The height (*H*, 1: 5,2 cm) is measured. The formula (ABC)/2 [$H \times AP \times T$)/2] is applied to calculate the hematoma volume, which is (5.2 cm $\times$ 5.5 cm $\times$ 5.1 cm)/2 = 73 cm^3. *A* anterior, *P* posterior, *L* left, *R* right, *S* superior, *I* inferior

of the angle of insonation, providing more accurate flow velocities.

Similar to TCD, the transtemporal is the main window and thus the first performed. In the transtemporal window, three main planes are recognized using TCCS: the mesencephalic, the diencephalic and the ventricular plane. The mesencephalic plane is characterized by central hypoechoic butterfly-shaped cerebral peduncles, surrounded by the hyperechoic basal cisterns (Fig. 11a). Angulating ten grades cephalad, the diencephalic plane is now recognized by the central two hyperechoic line corresponding to the third ventricle, the hypoechoic thalami on each side of the third ventricle and the hyperechoic pineal gland (Fig. 11b). With further cephalad angulation, the ventricular plane is now demarcated by the frontal horns of the lateral ventricles (Fig. 11c). The mesencephalic and diencephalic planes are commonly used for vascular diagnosis, because in these planes the Circle of Willis is found [15, 25] (Fig. 11d).

In the transforaminal window, a central hypoechoic structure is recognized, corresponding to the foramen magnum; color Doppler shows an inverted "v" normally coded blue, corresponding to the intracranial segment of the vertebral arteries and the basilar artery (Fig. 12).

The transorbitary window shows the anechoic globe and the echogenic retrobulbar area. On color Doppler, approximately at a depth of 40 mm, the ophthalmic artery (coded red) crosses the optic nerve (Fig. 13). At a depth of 80 mm, the carotid siphon can be investigated, as in TCD. The utility of this window also lies in the possibility of measuring the optic nerve sheath diameter (ONSD) for non-invasive assessment of intracranial pressure [15].

On color Doppler, the transcervical view shows a flow coded blue, corresponding to the ICA or the ECA; these flows must be differentiated using the PW Doppler with the criteria mentioned above (see Fig. 5 above).

Although the main use of TCCS is hemodynamic assessment, two-dimensional capabilities (and sometimes color Doppler) offer the possibility to detect relevant pathologic findings for the most common neurocritical care scenarios [26]. TCCS can be helpful in detecting intra-axial intracranial hematomas (i.e., intraparenchymal hematomas) and extra-axial intracranial hematomas (epidural and subdural),
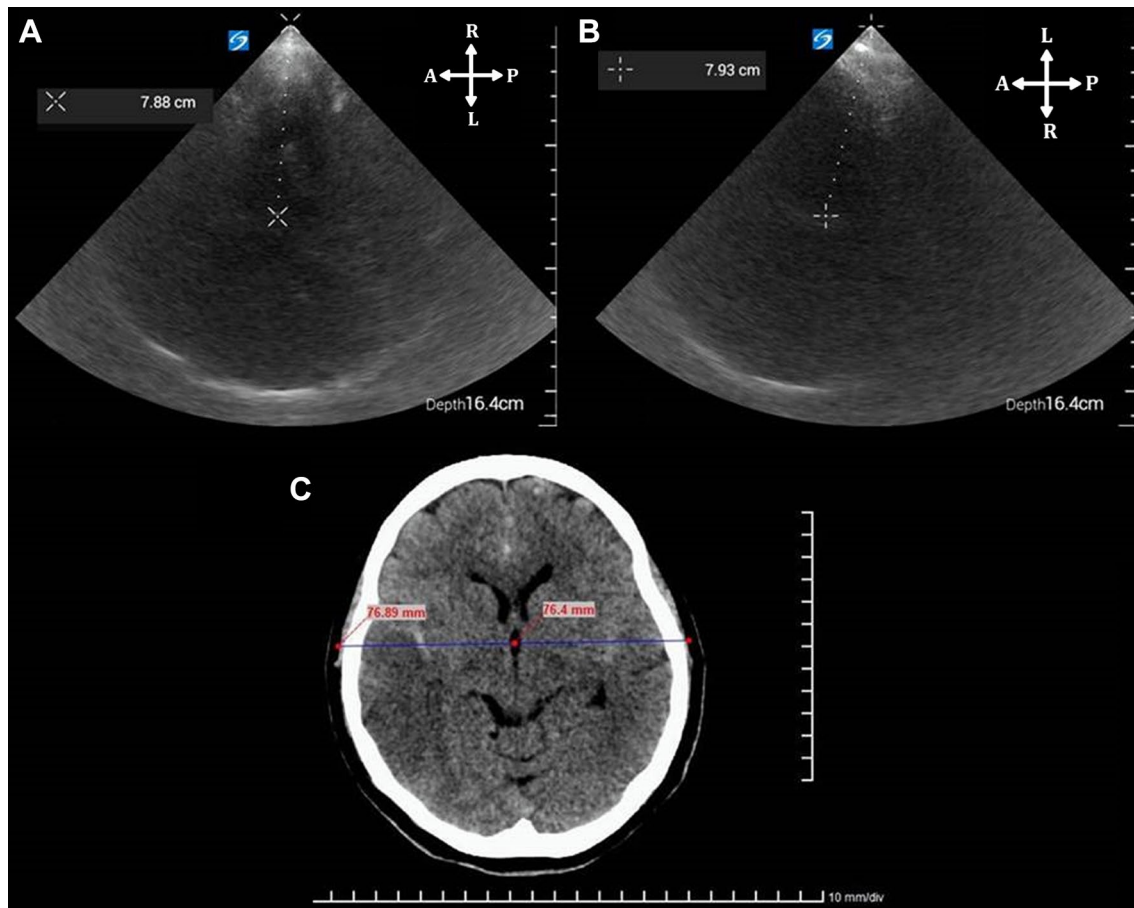
Fig. 16 Technique for measurement of MLS. *A* and *B* distances are obtained from the start of the ultrasound beam to the center of the third ventricle, bilaterally. **a** *A* distance is 78.8 mm (right transtem-poral view). *b* *B* distance is 79.3 mm (left transtemporal view). MLS = (*A* − *B*)/2. The MLS is negligible, measuring 0.25 mm left-ward, correlating with cranial CT in **c**

midline shift, hydrocephaly, cerebral tumors, cerebral aneurysms and arteriovenous malformations. Contrast-enhanced TCCS and three-dimensional TCCS are not widely available and are seldom used in the ICU. As previously mentioned, CEUS may improve detection of cerebral flows in non-conclusive TCD. In order of importance in neurocritical care, we now review the most useful applications of TCCS.

Intracranial hematomas

Acute (< 5 days) intra- and extra-axial hematomas present as hyperechoic masses [15, 26]. After 5 days, the hematomas become hypoechoic with a peripheral hyperechoic halo (Fig. 14). Detecting intracranial hematomas with TCCS depends principally on location more than on size; thus, deep hematomas (e.g., hypertensive bleeding in basal ganglia) are best recognized in comparison with lobar hematomas, such as parietal or frontal lobe hematomas. Reported sensibility and specificity for TCCS in detecting hematomas in hemorrhagic stroke are 94 and

95%, respectively, while the reported detection rate in extra-axial hematomas is 88% [15].

The main differential diagnoses of hematomas on TCCS are the arteriovenous malformations and cerebral tumors, which are also hyperechoic; thus, confirming the TCCS findings with a CT is mandatory when new bleeding is suspected.

An interesting application of TCCS is in detecting the expansion of hematoma; this has good correlation with the CT. This requires measuring the volume of the hematoma using both axial and coronal planes and calculating the volume using the formula: (*A* × *B* × *C*)/2 [15], where *A* corresponds to height, *B* to anteroposterior diameter and *C* to transverse diameter (Fig. 15).

Midline shift

The midline shift (MLS) is evaluated in the diencephalic plane. A first measurement ("*A*") is taken from the start of

the ultrasound beam to the center of the third ventricle. A second ("B") is taken in the same way by insonating from the contralateral side. MLS is calculated as $(A - B)/2$ (Fig. 16). A good correlation with CT has been demonstrated in several studies. An MLS > 2.5 mm on TCCS is considered significant and its detection is helpful in deciding the optimal time to perform a new TC [15, 27, 28].

In cases of decompressive craniectomies, cephalohematomas, skull fractures or evident cranial asymmetries, this method of measuring the MLS is inaccurate. Particularly for decompressive craniotomies, a direct method of measuring the MLS, with a good correlation with the CT, consists of insonating over the skull defect and measuring the deviation of the septum pellucidum in comparison with the midline given by the cerebral falci [29].

Hydrocephalus

Measurement of third ventricle dilation on TCCS has a good correlation with CT. For this application, a diencephalic plane is used—the third ventricle measured from inner border to inner border [28, 30]. Reference values are 4.8 ± 1.9 mm in patients younger than 60 years and 7.6 ± 2.1 mm in patients older than 60 years [31]. Ventricular dilation on TCCS does not seem to correlate well with the CT. This is mainly because of the large inclination of the ultrasound beam needed to visualize this structure. However, repeated measurements are of special value, as demonstrated by Kiputh et al. [32] in 37 adult patients with posthemorragic hydrocephalus, in which lumbar or external ventricular drainage was reopened or removed after repeatedly measuring the lateral ventricle diameters by TCCS.

Conclusions

Within a multimodal monitoring strategy, transcranial Doppler has an increasing role in the routine monitoring of neurocritical care patients. Since TCD is not invasive, is portable and does not emit ionizing radiation, this method can be initially considered for hemodynamic assessment and thus collaborating in inferring cerebral perfusion at patients' bedsides. In the case of TCCS, two-dimensional imaging may also contribute to diagnosis and follow-up. It is important to note that TCD must be used appropriately and that it does not exclude the use of other imaging techniques, such as CT. Finally, to the authors' knowledge, neither the basic TCD competencies nor the learning curve are defined for intensivists; thus, a competence-based curriculum is necessary and expected in the near future.

Compliance with ethical standards

Conflict of interest The authors have no conflict of interest to disclose.

Ethical approval All procedures performed in studies involving human participants were in accordance with the ethical standard of the institutional and/or national research committee and with the 1964 Helsinski declaration and its later amendments or comparable ethical standards.

Human and animal studies This article does not contain any studies with human participants or animals performed by any of the authors.

Informed consent Informed consent was obtained from all individual participants included in the article.

References

1. Le Roux P, Menon DK, Citerio G, Vespa P, Bader MK, Brophy GM, Diringer MN, Stocchetti N, Videtta W, Armonda R, Badjatia N, Böesel J, Chesnut R, Chou S, Claassen J, Czosnyka M, De Georgia M, Figaji A, Fugate J, Helbok R, Horowitz D, Hutchinson P, Kumar M, McNett M, Miller C, Naidech A, Oddo M, Olson D, O'Phelan K, Provencio JJ, Puppo C, Riker R, Robertson C, Schmidt M, Taccone F, Neurocritical Care Society, European Society of Intensive Care Medicine (2014) Consensus summary statement of the international multidisciplinary consensus conference on multimodality monitoring in neurocritical care: a statement for healthcare professionals from the neurocritical care society and the European society of intensive care medicine. Intensive Care Med 40(9):1189–1209
2. Lazaridis C, Robertson CS (2016) The role of multimodal invasive monitoring in acute traumatic brain injury. Neurosurg Clin N Am 27(4):509–517
3. Kirkman MA, Smith M (2016) Multimodality neuromonitoring. Anesthesiol Clin 34(3):511–523
4. Yuan Q, Wu X, Sun Y, Yu J, Li Z, Du Z, Mao Y, Zhou L, Hu J (2015) Impact of intracranial pressure monitoring on mortality in patients with traumatic brain injury: a systematic review and meta-analysis. J Neurosurg 122(3):574–587
5. Forsyth RJ, Raper J, Todhunter E (2015) Routine intracranial pressure monitoring in acute coma. Cochrane Database Syst Rev 11:CD002043
6. Dimitriou J, Levivier M, Gugliotta M (2016) Comparison of complications in patients receiving different types of intracranial pressure monitoring: a retrospective study in a single center in Switzerland. World Neurosurg 89:641–646
7. Karvellas CJ, Fix OK, Battenhouse H, Durkalski V, Sanders C, Lee WM, U S Acute Liver Failure Study Group (2014) Outcomes and complications of intracranial pressure monitoring in acute liver failure: a retrospective cohort study. Crit Care Med 42(5):1157–1167
8. Aaslid R, Markwalder TM, Nornes H (1982) Noninvasive transcranial Doppler ultrasound recording of flow velocity in basal cerebral arteries. J Neurosurg 57(6):769–774
9. Walter U (2012) Transcranial sonography of the cerebral parenchyma: update on clinically relevant applications. Perspect Med 1:334–343

10. Bartels E (2012) Transcranial color-coded duplex ultrasonography in routine cerebrovascular diagnostics. Perspect Med 1:325–330

11. Rasulo FA, De Peri E, Lavinio A (2008) Transcranial Doppler ultrasonography in intensive care. Eur J Anaesthesiol Suppl 42:167–173

12. Naqvi J, Yap KH, Ahmad G, Ghosh J (2013) Transcranial Doppler ultrasound: a review of the physical principles and major applications in critical care. Int J Vasc Med 2013:629378

13. D'Andrea A, Conte M, Cavallaro M, Scarafile R, Riegler L, Cocchia R, Pezzullo E, Carbone A, Natale F, Santoro G, Caso P, Russo MG, Bossone E, Calabrò R (2016) Transcranial Doppler ultrasonography: from methodology to major clinical applications. World J Cardiol 8(7):383–400

14. D'Andrea A, Conte M, Scarafile R, Riegler L, Cocchia R, Pezzullo E, Cavallaro M, Carbone A, Natale F, Russo MG, Gregorio G, Calabrò R (2016) Transcranial Doppler ultrasound: physical principles and principal applications in neurocritical care unit. J Cardiovasc Echogr 26(2):28–41

15. Blanco P, Blaivas M (2017) Applications of transcranial color-coded sonography in the emergency department. J Ultrasound Med 36(6):1251–1266

16. Abdo A, Pérez-Bernal J, Hinojosa R, Porras F, Castellanos R, Gómez F, Gutiérrez J, Castellanos A, Leal G, Espinosa N, Gómez-Bravo M (2015) Cerebral hemodynamics patterns by transcranial Doppler in patients with acute liver failure. Transplant Proc 47:2647–2649

17. Murillo-Cabezas F, Arteta-Arteta D, Flores-Cordero JM, Muñoz-Sánchez MA, Rincón-Ferrari MD, Rivera-Fernández MV, Alarcón-Cruz JC (2002) The usefulness of transcranial Doppler ultrasonography in the early phase of head injury. Neurocirugia (Astur) 13(3):196–208

18. Tegeler CH, Crutchfield K, Katsnelson M, Kim J, Tang R, Passmore Griffin L, Rundek T, Evans G (2013) Transcranial Doppler velocities in a large, healthy population. J Neuroimaging 23(3):466–472

19. Ract C, Le Moigno S, Bruder N, Vigué B (2007) Transcranial Doppler ultrasound goal-directed therapy for the early management of severe traumatic brain injury. Intensive Care Med 33(4):645–651

20. Ducrocq X, Hassler W, Moritake K, Newell DW, von Reutern GM, Shiogai T, Smith RR (1998) Consensus opinion on diagnosis of cerebral circulatory arrest using Doppler-sonography: task Force Group on cerebral death of the Neurosonology Research Group of the World Federation of Neurology. J Neurol Sci 159(2):145–150

21. Drudi FM, Giovagnorio F, Carbone A, Ricci P, Petta S, Cantisani V, Ferrari FS, Marchetti F, Passariello R (2006) Transrectal colour Doppler contrast sonography in the diagnosis of local recurrence after radical prostatectomy–comparison with MRI. Ultraschall Med 27(2):146–151

22. Cantisani V, Ricci P, Erturk M, Pagliara E, Drudi F, Calliada F, Mortele K, D'Ambrosio U, Marigliano C, Catalano C, Marin D, Di Seri M, Longo F, Passariello R (2010) Detection of hepatic metastases from colorectal cancer: prospective evaluation of gray scale US versus SonoVue® low mechanical index real time-enhanced US as compared with multidetector-CT or Gd-BOPTA-MRI. Ultraschall Med 31(5):500–505

23. Rafailidis V, Charitanti A, Tegos T, Destanis E, Chryssogonidis I (2017) Contrast-enhanced ultrasound of the carotid system: a review of the current literature. J Ultrasound 20(2):97–109

24. Seidel G, Meairs S (2009) Ultrasound contrast agents in ischemic stroke. Cerebrovasc Dis 27(Suppl 2):25–39

25. Blanco P (2016) Transcranial color-coded duplex sonography: another option besides the blind method. J Ultrasound Med 35(3):669–671

26. Blanco P (2015) Cerebral circulatory arrest detected by transcranial color-coded duplex sonography: a feasible diagnosis for intensivists. J Ultrasound Med 34(7):1337–1340

27. Blanco P, Matteoda M (2015) Images in emergency medicine. Extra-axial intracranial hematoma, midline shift, and severe intracranial hypertension detected by transcranial color-coded duplex sonography. Ann Emerg Med 65(2):e1–e2

28. Llompart Pou JA, Abadal Centellas JM, Palmer Sans M, Pérez Bárcena J, Casares Vivas M, Homar Ramírez J, Ibáñez Juvé J (2004) Monitoring midline shift by transcranial color-coded sonography in traumatic brain injury. A comparison with cranial computerized tomography. Intensive Care Med 30(8):1672–1675

29. Caricato A, Mignani V, Bocci MG, Pennisi MA, Sandroni C, Tersali A, Antonaci A, de Waure C, Antonelli M (2012) Usefulness of transcranial echography in patients with decompressive craniectomy: a comparison with computed tomography scan. Crit Care Med 40(6):1745–1752

30. Seidel G, Gerriets T, Kaps M, Missler U (1996) Dislocation of the third ventricle due to space-occupying stroke evaluated by transcranial duplex sonography. J Neuroimaging 6(4):227–230

31. Seidel G, Kaps M, Gerriets T, Hutzelmann A (1995) Evaluation of the ventricular system in adults by transcranial duplex sonography. J Neuroimaging 5(2):105–108

32. Kiphuth IC, Huttner HB, Struffert T, Schwab S, Köhrmann M (2011) Sonographic monitoring of ventricle enlargement in posthemorrhagic hydrocephalus. Neurology 76(10):858–862